# Automatic coronary artery calcium scoring from unenhanced-ECG-gated CT using deep learning

Nicolas Gogin, Mario Viti, Luc Nicodème, Mickaël Ohana, Hugues Talbot, Umit Gencer, Magloire Mekukosokeng, Thomas Caramella, Yann Diascorn, Jean-Yves Airaud, et al.

▶ **To cite this version:**

Nicolas Gogin, Mario Viti, Luc Nicodème, Mickaël Ohana, Hugues Talbot, et al.. Automatic coronary artery calcium scoring from unenhanced-ECG-gated CT using deep learning. Diagnostic and Interventional Imaging, 2021, 102 (11), pp.683-690. 10.1016/j.diii.2021.05.004 . hal-03500506

**HAL Id: hal-03500506**
**https://hal.science/hal-03500506v1**

Submitted on 22 Dec 2021

**HAL** is a multi-disciplinary open access archive for the deposit and dissemination of scientific research documents, whether they are published or not. The documents may come from teaching and research institutions in France or abroad, or from public or private research centers.

L'archive ouverte pluridisciplinaire **HAL**, est destinée au dépôt et à la diffusion de documents scientifiques de niveau recherche, publiés ou non, émanant des établissements d'enseignement et de recherche français ou étrangers, des laboratoires publics ou privés.

# Automatic coronary artery calcium scoring from unenhanced-ECG gated CT by using deep learning

**Short title**:

**ABSTRACT**

**Purpose**

**Material and methods**

.

**Results**:

**Conclusions**:

**KEYWORDS:** Multidetector computed tomography;

# Automatic coronary artery calcium scoring from CT using deep learning

Nicolas Gogin[(a)], Mario Viti[(a,c)], Luc Nicodème[(a)], Mickaël Ohana[(b)], Hugues Talbot[(c)], Umit Gencer[(d)], Magloire Mekukosokeng[(e)], Thomas Caramella[(f)], Yann Diascorn[(f)], Jean-Yves Airaud[(g)], Marc-Samir Guillot[(d)], Zoubir Bensalah[(h)], Caroline Dam Hieu[(a)], Bassam Abdallah[(a)], Imad Bousaid[(i)], Nathalie Lassau[(i,j)], Elie Mousseaux[(d)]

(a): GE Healthcare, Buc, France
(b): CHU Strasbourg, Service de Radiologie, Strasbourg, France
(c): CentraleSupélec, Université Paris-Saclay, CentraleSupélec, Inria, Gif-sur-Yvette, France
(d): Radiology Department, APHP, Hôpital Européen Georges Pompidou, Georges Pompidou, Université de Paris, PARCC, INSERM, France.
(e): Centre Hospitalier de Douai, Douai, France
(f): Institut Arnault Tzanck, Saint Laurent du Var, France
(g): Service Scanner, Polyclinique Inkermann, Niort, France
(h): Radiology Department, Centre Hospitalier de Perpignan, Perpignan, France.
(i): Imaging Department, Gustave Roussy, Université Paris -Saclay, Villejuif, France
(j): Biomaps, UMR 1281 INSERM, CEA, CNRS, Université Paris-Saclay, Villejuif, France

***Abstract—***

*Rationale and Objectives*: The purpose of this study was to develop and validate an algorithm that can automatically estimate the amount of coronary artery calcium (CAC) from non-enhanced ECG-gated computed tomography (CT) cardiac volume acquisitions by using multiple convolutional neural networks (CNN).
*Materials and Methods:* Our method used an ensemble of 5 CNN with 3D U-Net architecture trained on a database of 783 CT examinations to detect and segment coronary artery calcifications in a 3D volume. The Agatston score, the conventional CAC scoring, was then computed slice by slice from the resulting segmentation mask and compared to the ground truth manually estimated by radiologists.
The quality of the estimation was assessed with the Concordance Index (C-index) on a separate testing set of 98 independent CT examinations.
*Results*: The final ensemble model yields a C-index of 0.951 on the testing set. The remaining errors of the method were mainly observed on small-size and/or low-density calcifications, or calcifications located near the mitral valve or ring. Our model was also compared to other methods from the literature showing state-of-the-art performance for CAC quantification.
*Conclusion:* The deep learning-based method we proposed to compute automatically the CAC score from a non-enhanced ECG-gated cardiac CT is fast, robust and could improve workflow efficiency, eliminating the time spent on manually selecting coronary calcifications to compute the Agatston score.

***Keywords— Tomography, X-ray computed, Deep learning, Coronary Artery Disease, Convolutional neural networks (CNN)***

**ABBREVIATIONS:**

CAD: Coronary artery disease
CAC: Coronary Artery Calcium
CNN: Convolutional Neural Networks
FCNN: Fully Convolutional Neural Networks
HU: Hounsfield Units
SFR: the French Radiology Society

## Introduction

Coronary artery disease (CAD) is one of the leading causes of mortality in the world. Coronary Artery Calcium (CAC) has been shown to be associated with the presence of CAD and to be a strong and independent predictor of cardio-vascular events and mortality [1]. CAC can be quantified with low dose ECG-gated non enhanced CT acquisition, by using standardized parameters and notably a tube voltage of 120 kV and a series of 2.5 to 3 mm thick slices covering the entire cardiac volume.
In clinical practice, the CAC burden is estimated by the Agatston score, which has been widely validated in numerous studies in estimating cardiovascular risk [2]. Such Agatston score is computed from 2D axial connected components above 130 Hounsfield Units (HU) that are manually or semi automatically identified as coronary calcification by the radiologist. A manual intervention is often required to validate a segmentation made beforehand by a software, which exposes, beyond the time spent, to measurement variability depending on the software and the experience of the operator. According to several guidelines [3], this score is a reliable tool to classify patients into 5 classes for risk assessment and to guide follow-up preventive strategy and testing. Several recent studies report different experiences in automating the procedure of segmentation and quantification of the CAC burden, using different deep learning approaches.
Indeed, in the last few years semantic segmentation architectures were used to predict dense segmentation maps by extending Convolutional Neural Networks (CNN) to Fully Convolutional Neural Networks (FCNN) [4]. They were first applied to 2D biomedical imagery with the so-called U-Net [5] and later with a straightforward extension to 3D and 4D V-Net [6]. The objective of our study was to propose and validate a new fully automated method of segmentation and quantification of CAC burden based on a customized version of these architectures in the context of the data challenge organized in 2020 by the French Radiology Society (SFR).

## Materials and Methods

### *Patient Population and Database*

The data set of the SFR's data challenge 2020 is composed of 3 different batches of CT acquisitions collected from different clinical sites and provided at different stages of the data challenge. A first batch of 100 CT examinations was made available at the beginning of the data challenge (J1 data set), then a second larger batch of 322 CT examinations was released two days before the end of the challenge (J2 dataset). A final dataset of 98 CT examinations (J3 dataset) was given during the last day of the data challenge to be used as a test set to evaluate in one hour the results submitted by all the participants to the challenge.
Patients included in this final dataset were classified at intermediate cardiovascular risk group, based on the risk score index, with an average age of 60 years plus or minus 13 years (range 43-84 years). However, based on the manually calculated Agatston score, and unbeknownst to the challenge participants, the

distribution of classes was homogeneous as nearly 20% of the subjects were selected to represent each class from A to E.
All ECG gated CT exams were acquired without contrast injection, by using tube voltage of 120 KeV and a slice spacing of 2.5 or 3.0 millimetres. The need for informed consent from the patient was waived by the national commission in charge of data protection and the relationship between computer science and freedom in France (CNIL). Furthermore, the SFR ensure the data protection to radiologists wishing to participate in the challenge by providing an automatic anonymization process integrated into the platform for loading images.
The competition organisers ensured a good distribution of the examinations between 4 CT vendors in order to avoid results depending on a manufacturer specific type of image. They also accompanied each patient image series with a list of 3d positions of each coronary calcification manually and specifically marked by a radiologist expert in the field. Finally, based on the radiologist results, they assigned the following standard risk categories for each patient: A, B, C, D or E when Agatston score was zero, 1-10, 11-100, 101-400, > 400, respectively.
The distribution of Agatston score for each subset is provided in Figure 1. An additional 361 annotated CT acquisitions (AD dataset) coming from our internal database was also used as training data.

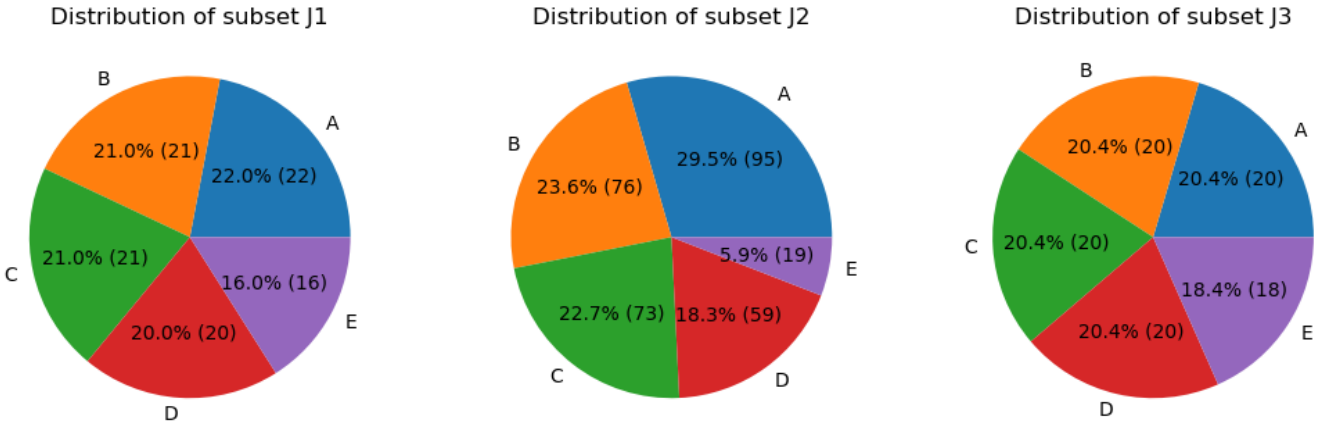


Figure 1: Distribution of Agatston risk score for each batch of data

As an additional validation step, we also evaluated the model on the public test set of the orCaScore challenge to assess the capacity of our model to generalize on external data independent from the SFR challenge data distribution [7]. The orCaScore challenge provides a public benchmark to evaluate and compare different methods for CAC scoring. This public dataset consists of non-contrast enhanced ECG-triggered cardiac CT acquired on CT scanners from four different vendors from four different hospitals. The training data provided with this framework was not used in this study, only the 40 test CT volumes were used as external test set.

## *AI methodology*

*Overview*
Our approach consists in training an ensemble of 3D U-Net models that outputs a binary segmentation mask of calcifications. The Agatston score (AS) is then computed by 2d connected component analysis performed on each slice of the mask using the following formula:

$$Agatston\ Score = \sum_i \sum_j a_{ij} d_{ij} \frac{\Delta z}{3}$$

Where $a_{ij}$ is the area of the $j^{th}$ 2d connected component (of at least 3 voxels) on the $i^{th}$ axial slice, $d_{ij}$ is a density factor determined by the maximum attenuation in this connected component ($130-199\,HU: 1, 200-299\,HU: 2, 300-399\,HU: 3, \geq 400\,HU: 4$), and $\Delta z$ is the axial thickness of the acquisition in millimeters.

*Ground truth generation*

For each CT volume of the training set, we created a ground truth derived from the provided annotations. This ground truth is a binary mask of calcifications. This process was performed automatically by selecting the connected components of voxels above 130 HU connected to the calcification 3d positions provided in the annotation. To ensure the quality of the segmentation mask, the Agatston score was then computed from the mask and compared to the original Agatston score category. In case of discrepancy between the two scores, the masks were reviewed, and manually corrected if needed.

*Pre-processing*

Each CT volume was first downsampled to an isotropic resolution of either 2.5 mm or 3 mm (depending on the original slice spacing). As an effect of the downsampling, the information of low-density calcifications could be lost in the low-resolution image. In order to restore this information, intensities above 130 HU in the original image were enhanced in the downsampled image. Finally, the processed volume was clipped below -300 HU and above 800 HU, and linearly normalized between 0 and 1. Corresponding ground truth masks were also downsampled at the same resolution.

*Model architecture*

Each model was built on a 3D U-Net architecture with a depth of 4 levels and 16 initial filters. Each convolution layer used residual connections, exponential linear unit (ELU) activation and batch normalization. The number of filters was doubled after each max pooling layer in the encoding path, while in the decoding path, the number of filters was symmetrically decreased by a factor 2 after each up-sampling layer. The detailed architecture of the network is provided in Figure 2. A majority vote per voxel among the 5 different outputs of each model was used as the final prediction of the calcification mask.

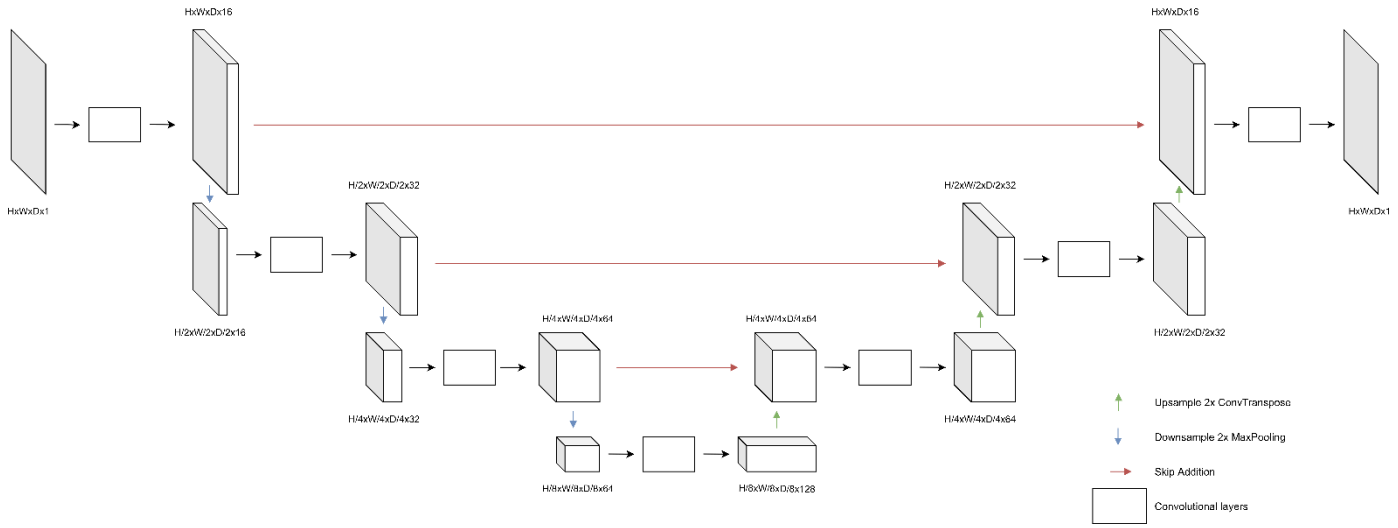


Figure 2: Model architecture

*Training*

The training of each U-Net model was done from scratch with Adam optimizer on the Dice loss function. A validation set of 20 exams from J1 was used to select the best epoch during training. The training process was done with TensorFlow version 1.14 in Python 3.6, on a NVIDIA® GV100-32GB GPU. We considered 3 different data subsets for training: J1, J1+J2, J1+J2+AD, and trained independently 5 models for each of these subsets.

*Post-processing*

The ensembled model was obtained by majority vote per voxel among the different outputs of the 5 models trained on the same training subset. The predicted mask was then upsampled to the original resolution and intensities were thresholded at 130HU.

*Testing and validation*

For each test volume, the model predicted a calcification mask on which the Agatston score was further calculated. The resulting Agatston score risk category was then compared to the ground truth for each volume of the test set. Two metrics were computed to evaluate the method: category accuracy and C-index. The category accuracy gives the percentage of correct risk category in the evaluation set. The C-index or Harrel index measures the proportion of concordant pairs divided by the total number of possible evaluation pairs: C-index = $\frac{\#\ concordant\ pairs}{\#\ all\ pairs} = \frac{\#\ \{\ (i,j)\ s.t.\ p_i<p_j\ and\ t_i<t_j\ \}}{\binom{n}{2}}$ where $p_i$ is the predicted risk category, $t_i$ is the true risk category and $n$ is the number of elements to compare. The C-index lies between 0.5 (random prediction) and 1 (all risk category correctly predicted).

## Results

The performance of the different models is presented in Table 1 and Figure 3, showing the average performance obtained with a single model compared to the performance of the ensembled model for the different training sets considered. As expected, the C-index improved with the size of the training set from 0.9391, 0.9437 to 0.9509 when using J1, J1+J2 and J1+J2+AD data sets respectively. The final model was trained on the full training set of 783 exams (J1+J2+AD).

Table 1: Performance of each model. 1 model vs Ensembled model.
For 1 model, average and standard deviation across the 5 trained models are reported.

| **Method** | **Metrics** | |
|---|---|---|
| | **C-index** | **category accuracy** |
| 1 model trained on J1 (average performance) | **0.932 (std=0.008)** | **0.832 (std=0.010)** |
| Ensemble of 5 models trained on J1 | **0.939** | **0.847** |
| 1 model trained on J1 + J2 (average performance) | **0.943 (std=0.005)** | **0.849 (std=0.015)** |
| Ensemble of 5 models trained on J1 + J2 | **0.944** | **0.847** |
| 1 model trained on J1 + J2 + AD (average performance) | **0.949 (std=0.006)** | **0.864 (std=0.010)** |
| Ensemble of 5 models trained on J1 + J2 + AD (Final) | **0.951** | **0.857** |

In addition, we observed that ensembling 5 different models improved the performance in terms of C-index compared to the average performance of a single model. On the models trained with the full set, we have seen a small degradation in accuracy with the ensembled model, while the C-index is improved. The two metrics are indeed not equivalent. With the C-index, a large error on the predicted class has more influence on the metric than a small one, whereas this predicted class difference is weighted equally with the accuracy measure. Thus, the ensemble model made slightly more errors than the average model, but the magnitude of the errors was smaller.

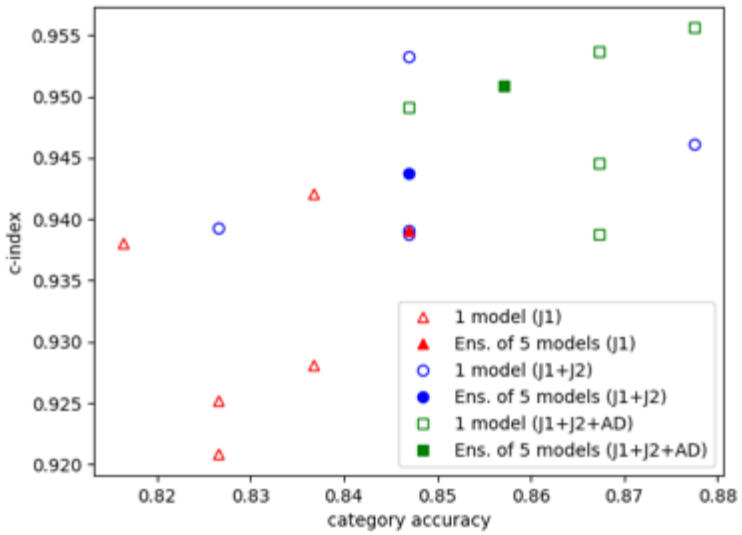


Figure 3: C-index vs accuracy for different models evaluated on the test set (J3).

This observation was confirmed by the confusion matrix (Figure 4) which gives the distribution of errors across the different patient risk categories based on the Agatston score. With the final model, most of the errors were distributed near the diagonal, corresponding to off-by-one errors. Some recurring failure patterns were observed: small low-density calcifications could be missed (6 errors where A is predicted instead of B), and in a few cases some coronary calcifications were mistaken for calcifications on the mitral valve. This is illustrated in Figure 5 where examples of both successful and failed predictions are presented. These error patterns could indicate the type of exams that should be added in the training set in order to further increase the performance.

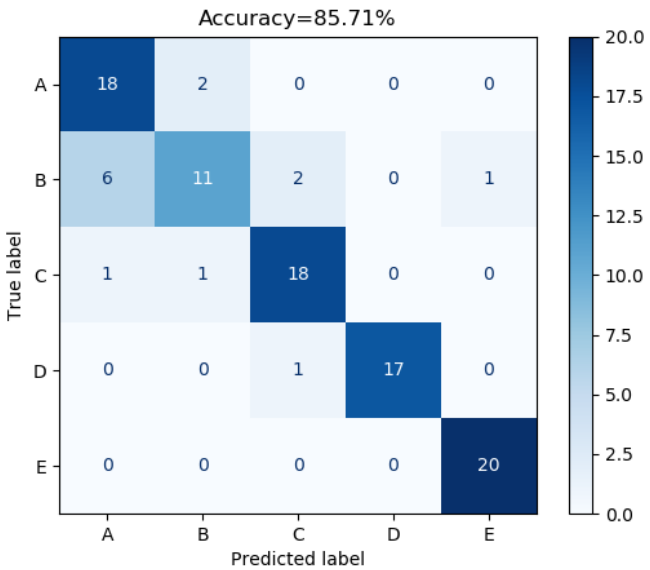


Figure 4: Confusion Matrix for the Risk Score of the final prediction on the test set (J3)

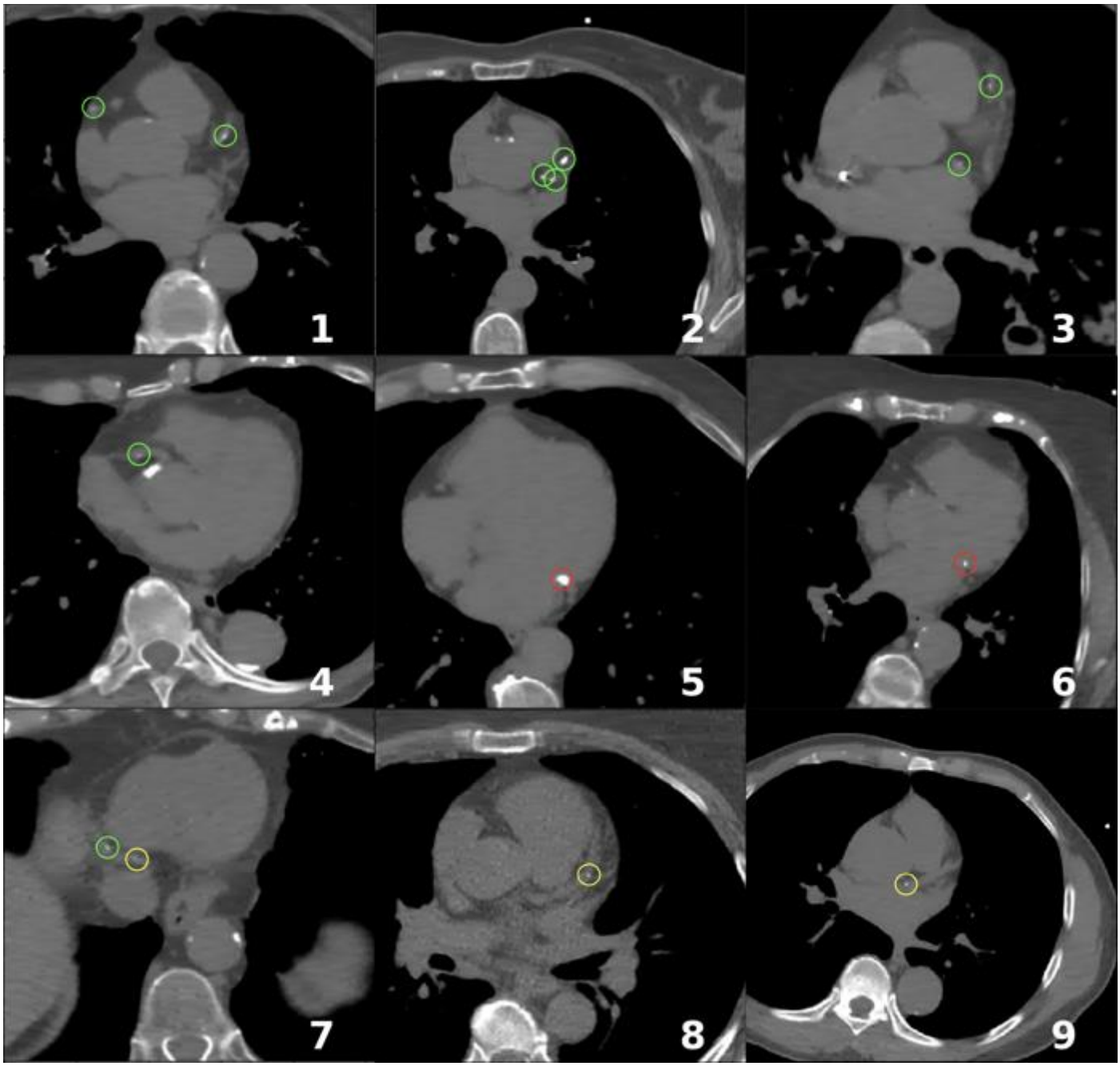


Figure 5: Examples of prediction by the final ensembled model. Green circles are true positives, red circles are false positives (false detection), yellow circles are false negatives (missed calcification). 1-4 are examples of correct predictions, 5-9 are examples of incorrect predictions with either false detections or missed detections. Examples 5, 6 and 9 are typical examples of the confusion made between mitral valve calcifications and coronary artery calcifications.

Finally, the final model was evaluated on the public benchmark of OrcaScore [7] and yielded a F1-score of 0.974 with an accuracy of 0.975 on the 40 CT volumes of the test set, ranking first in the leaderboard at the

time of the submission. This confirmed our model can generalize well on a wide range of non-enhanced ECG-gated cardiac CT examinations.

## DISCUSSION

Our method based on an ensemble of five 3D U-Net models to detect dense segmentation maps [8] has obtained good fully automated detection and quantification of the Agatston score. Indeed, our method was able to correctly classify the cardiovascular risk category in 86% of the 98 subjects of the validation database according to the Agatston's score level, quantified manually and conventionally by trained operators. As shown in the confusion matrix of the figure 4, a class discrepancy was observed in only 14 subjects, and since the amplitude of this discrepancy was low and =<1 class on 13 of these subjects, the c-index obtained with our method was 95%. We have also shown here the importance of the volume of the training data base of the different CNN models taken alone or combined on the final result.

In these conditions, it is not surprising to see that AI model proposals published in 2018 on a training data base of 1744 ECG gated CT acquisition dedicated for CAC scoring [9] now obtain results very close to those obtained manually by operators trained to detect the coronary calcium score when these databases have been diversified by different types of scanner and when these training databases are much larger [10]. In this large study including 7240 participants with a wide range of CT examination with ECG gated CAC scoring CT, diagnostic chest CT, PET attenuation correction CT and radiation therapy CT, the deep learning solution was tested on 4324 CT examination to obtain a weighted kappa value of 0.90 for all test CT scans and ICC yielded 0.79–0.97 for CAC across the range of different types of CT examinations.

From a methodological point of view, different methods have been proposed in the automated detection and analysis of CAC score on CT. A method based on an ensemble of pairs of CNNs obtained 83% of accuracy in predicting patients CAC score risk class by using only the enhanced CT when the classification requested to the algorithm was only 4 classes instead of 5 [11]. If classes B and C are grouped together in a single class (CAC score from 1 to 100) as it is often suggested in clinical practice in non-diabetic subjects, the accuracy of our solution could also increase from 84 to 94%. Another approach makes use of fuzzy features and atlas-based information in conjunction with Random Forest Models to exploit the available data at best and get accurate quantification and branch-wise location of CAC and only the non-enhanced-CT images are required [12]. To produce a more accurate segmentation of coronary artery, another method has been suggested to automatically detect calcified lesions on the non-enhanced CT images, but the segmentation of the aorta, the heart and coronary arteries was required and obtained by using associated contrast CT images [13]. Because of its relevance in CAD screening in a population of smokers, another deep learning method has been tested on the NLST (National Lung Screening Trial) [14]. This method uses of a 2-stage FCNN prediction to quantify branch-wise calcifications using the sole non-enhanced CT examination [9]. This method previously trained on manual and segmental labeling of calcified coronary lesion per coronary artery in a subset population of the NLST patients was further tested on multiple cardiac CT protocols as previously mentioned [10]. Finally, a last interesting method still based on CNN [15] was trained on NLST data set using only the CAC score information as supervision. The method employs two CNNs, one for registration to align the input images to an atlas image made from cardiac CTs and one for direct CAC score prediction using regression. This second CNN operates on 2d slices and does not use the information across slices which according to the authors may account for some incorrect identification of CAC near the coronary artery ostia.

By contrast our approach is fully 3D and therefore is capable of better using the information across adjacent slices to identify CAC. To maintain a large receptive field while limiting the depth of the CNN, we chose to train our model on low-resolution versions of the CT volumes using a single standard U-Net architecture, which led to a cost-effective training and inferencing process (less than 2 seconds per examination). The

performance obtained with our model on the orCaScore test set was very close to the other top performing methods evaluated with this framework [12,13,15].

The limitation of our work presented here was that only dedicated non-enhanced-ECG-gated CT scans for calcium score were trained and evaluated. Given the value of the CAC score in detecting subjects at high cardiovascular risk who require primary prevention, it would be useful in future studies to test and validate this method on a wider range of CT acquisition performed for routine examinations for lung disease.

## CONCLUSION

We have presented here a method based on an ensemble of five customized U-Net models trained on a database of 783 exams to compute the Agatston Score from non-enhanced CT scan. The performance achieved with our method to quantify CAC score was very close from those obtained by the best deep learning methods recently published in the literature. Thus, our deep learning method could improve clinical workflow efficiency as radiologists would not need to spend time tediously segmenting coronary calcifications by hand.

### HUMAN RIGHTS

The authors declare that the work described has been carried out in accordance with the Declaration of Helsinki of the World Medical Association revised in 2013 for experiments involving humans.

### INFORMED CONSENT AND PATIENT DETAILS

The authors declare that this study does not contain any personal information that could lead to the identification of the patient(s).

### FUNDING

This work did not receive any grant from funding agencies in the public, commercial, or not-for-profit sectors.

### AUTHOR CONTRIBUTIONS

All authors attest that they meet the current International Committee of Medical Journal Editors (ICMJE) criteria for Authorship. All the authors had fully participated to the study and approved the final draft.

### AUTHORS CREDITS

Nicolas Gogin: Methodology, Investigation, Software, Validation, Formal analysis, Writing - Original Draft, Writing – Review & Editing, Supervision
Mario Viti: Methodology, Investigation, Software, Validation, Formal analysis, Writing - Original Draft, Writing – Review & Editing
Luc Nicodème: Methodology, Investigation, Software, Validation, Formal analysis, Writing - Original Draft, Writing – Review & Editing
Mickaël Ohana: Review & Editing, Data Curation
Hugues Talbot: Review & Editing
Umit Gencer: Data Curation
Magloire Mekukosokeng: Data Curation
Thomas Caramella: Data Curation
Yann Diascorn: Data Curation

Jean-Yves Airaud: Data Curation
Marc-Samir Guillot: Data Curation
Zoubir Bensalah: Data Curation
Caroline Dam Hieu: Data Curation, Software
Bassam Abdallah: Data Curation, Software
Imad Bousaid: Project administration, Resources
Nathalie Lassau: Project administration, Resources
Elie Mousseaux: Project administration, Resources, Writing - Original Draft, Review & Editing, Supervision

ACKNOWLEDGEMENTS

We would like to thank the Société Francaise de Radiologie for the opportunity to participate in these challenges during the Journées Francophones de Radiologie. We would like to thank Gustave-Roussy for the resources mobilized and the data hosting.

DISCLOSURE OF INTEREST

NG, MV, LN, CD, BA are employees of GE Healthcare. The other authors declare that they have no competing interest.

[1] Budoff M, Mayrhofer T, Ferencik M et al Prognostic Value of Coronary Artery Calcium in the PROMISE Study (Prospective Multicenter Imaging Study for Evaluation of Chest Pain). *Circulation 2017*,136 (21): 1993-2005; doi: 10.1161/CIRCULATIONAHA.117.030578.

[2] Agatston A, Janowitz W, Hildner F et al. Quantification of coronary artery calcium using ultrafast computed tomography," *JACC 1990*, 15(4):, 827-832. doi: 10.1016/0735-1097(90)90282-T.

[3] Valensi P, Henry P, Boccara F, et al Risk stratification and screening for coronary artery disease in asymptomatic patients with diabetes mellitus: Position paper of the French Society of Cardiology and the French-speaking Society of Diabetology. *Diabetes Metab 2020.* doi: 10.1007/s00330-020-07417-0.

[4] Weikert T, Francone M, Abbara S et alMachine learning in cardiovascular radiology: ESCR position statement on design requirements, quality assessment, current applications, opportunities, and challenges. *Eur Radiol.2020*.doi: 10.1016/j.diabet.2020.08.002.

[5] Ronneberger O, Fischer P, Brox T et al U-Net: Convolutional Networks for Biomedical Image Segmentation , *Medical Image Computing and Computer-Assisted Intervention -- MICCAI 2015. Lecture Notes in Computer Science*, 9351, 234-241

[6] Milletari F, Navab N, Ahmadi S et al V-Net: Fully Convolutional Neural Networks for Volumetric Medical Image Segmentation, *Fourth International Conference on 3D Vision (3DV),2016* 565-571 doi:10.1109/3DV.2016.79.

[7] Wolterink J M, Leiner T, de Vos B D, Coatrieux J L, Kelm B M and Kondo S.An evaluation of automatic coronary artery calcium scoring methods with cardiac CT using the orCaScore framework. *Med. Phys.2016*,43, (5),2361. doi: 10.1118/1.4945696. PMID: 27147348.

[9] Lessmann N, van Ginneken B, Zreik M, de Jong P D and de Vos B D.Automatic Calcium Scoring in Low-Dose Chest CT Using Deep Neural Networks With Dilated Convolutions. *IEEE Transactions on Medical Imaging* 2018; 37, 615-625. doi: 10.1109/TMI.2017.2769839.

[10] van Velzen S, Lessmann N, Velthuis B et al. Deep Learning for Automatic Calcium Scoring in CT: Validation Using Multiple Cardiac CT and Chest CT Protocols. *Radiology 2020*.295 ( 1),66-79. doi: 10.1148/radiol.2020191621.

[11] Wolterink J, Leiner T, de Vos B, van Hamersvelt R, Viergever M and Išgum I.Automatic coronary artery calcium scoring in cardiac CT angiography using paired convolutional neural networks. *Med Image Anal 2016, 34*, 123-135 doi: 10.1016/j.media.2016.04.004.

[12] Durlak F, Wels M, Schwemmer C et al, Growing a Random Forest with Fuzzy Spatial Features for Fully Automatic Artery-Specific Coronary Calcium Scoring, *Machine Learning in Medical Imaging. MLMI 2017. Lecture Notes in Computer Science*, 10541, 27-35 doi:10.1007/978-3-319-67389-9_4.

[13] Yang G, Chen Y, Ning X, Sun Q, Shu H and Jin C, "Automatic coronary calcium scoring using noncontrast and contrast CT images," *Med Phys 2016,* 43, (5),2174. doi: 10.1118/1.4945045.

[14] The National Lung Screening Trial Research Team.Reduced lungcancer mortality with low-dose computed tomographic screening.*New England Journal of Medicine 2011,* 365(5),395-409 doi:10.1056/NEJMoa1102873

[15] de Vos BD, Wolterink J M, Leiner T, de Jong P A, Lessmann N and Isgum I, "Direct Automatic Coronary Calcium Scoring in Cardiac and Chest CT," *IEEE Transactions on Medical Imaging 2019* 38, (9),2127–2138. doi: 10.1109/TMI.2019.2899534.